into cytosolic compartment from the membrane bound form of p35 [24], resulting in hyperactivation of Cdk5. In contrast, Cdk5 shows protective activity against Huntington's disease (HD), which is one of the polyQ neurodegenerative disorders [1,17,21]. It will be interesting to determine whether Cdk5 has protective activity against the cytotoxicity of other polyQ proteins.

The examination of the amino acid sequence of ataxin-2 revealed the presence of 47 (S/T)P possible Cdk5 phosphorylation sites, with two (S/T)PX(K/R) best consensus sequences. We hypothesized that ataxin-2 is a substrate of Cdk5 and examined its phosphorylation by Cdk5 using a cultured-cell overexpression system.

## 2. Methods

### 2.1. Antibodies and chemicals

The anti-p35/p25 C19 and anti-Cdk5 C8 antibodies were obtained from Santa Cruz Biotechnology (Santa Cruz, CA). The anti-myc 4A6 antibody was obtained from Millipore (Billerica, MA). The anti-GFP antibody was purchased from Roche Diagnostics (Basel, Switzerland). The anti-actin antibody was purchased from Sigma (St Louis, MO). Horseradish peroxidase (HRP)-conjugated goat anti-mouse IgG, alkaline phosphatase (AP)-conjugated goat anti-mouse IgG, and HRP-conjugated swine anti-rabbit IgG were purchased from Dako (Glostrup, Denmark). Phos-tag acrylamide was obtained from Wako (Osaka, Japan). Benzyloxycarnonyl-leucyl-leucyl-leucinal (MG132) was obtained from the Peptide Institute (Osaka, Japan).

### 2.2. Mammalian cell expression vectors

Mouse p25-myc, mouse HA-Cdk5, the kinase-negative (kn) K33T mutant of Cdk5 (knCdk5) were reported previously [3]. GFP-tau was constructed by inserting human tau cDNA (1N4R) [11] at the BglII/SalI site of pEGFP-C1 vector (Invitrogen). Human ataxin-2 was amplified from a human fetal cDNA library by polymerase chain reaction (PCR) using 5′-AGATCTATGCGCTCAGCGGCCGCAGCTCCT-3′ and 5′-GCTGACCAACTGCTGTTGGTGGTGGGCTTG-3′ as forward and reverse primers, and was inserted at the BglII/SalI site of pGEM-T easy (Promega, Madison, WI). The clone obtained was ataxin-2-22Q. GFP-fusion was constructed by insertion of ataxin-2-22Q into a pEGFP-C1 vector. The CAG repeat tract was expanded as reported previously [6]. GFP-tagged ataxin-2 fragments were constructed by PCR using pEGFP-C1-ataxin-2 as a template. The GFP-tagged N-terminal fragment (NF, amino acids 1–507) of ataxin-2 was constructed by PCR using pEGFP-human ataxin-2 as a template and 5′-TAAGTCGACGGTACCGCG-3′ and 5′-CGGGATCCTTATCCCCAGGATATGACTTCTCT-3′ as forward and reverse primers. The GFP-tagged C-terminal fragment (CF, amino acids 906–1313) was constructed similarly using 5′-GCTGAGCAAGTTAGGAAA-3′ and 5′-AGATCTGAGTCCGGACTT-3′ as forward and reverse primers. The GFP-tagged middle fragment (MF, amino acids 508–905) was constructed from the GFP-NF-MF fragment, which was once constructed by PCR using 5′-CGGGATCCTTATCCCCAGGATATGACTTCTCT-3′ and the reverse primer for NF, by secondary PCR using 5′-AGTGGGAGACAGAATT-3′ and 5′-AGATCTGAGTCCGGACTT-3′ as forward and reverse primers. All plasmid vectors were verified by DNA sequencing.

### 2.3. Cell culture, transfection, immunoblotting, quantification and statistical analysis

COS-7 cell culture and transfection were performed as described previously [3]. COS-7 cells were lysed by sonication in Laemmli sample buffer. Laemmli sodium dodecyl sulfate polyacrylamide gel electrophoresis (SDS-PAGE) was carried out using 6% or 12.5% polyacrylamide gels [4], and Phos-tag SDS-PAGE was performed using 5% polyacrylamide gels containing 50 μM Phos-tag and 100 μM $MnCl_2$ [13,18]. Immunodetection after blotting was performed using a Millipore Immobilon chemiluminescent HRP substrate (Millipore) and an ECL system (GE Healthcare, Piscataway, NJ) or BCIP/NBT phosphatase substrate kit (KPL, Gaithersburg, MD). Quantification was performed with image-J software, and the statistical significance of data was determined by one-way analysis of variance with Tukey's post hoc test.

### 2.4. Immunoprecipitation and in vitro phosphorylation by Cdk5–p25

GFP-tagged proteins, ataxin-2, its fragments or tau, were expressed in COS-7 cells and immunopurified using an anti-GFP antibody [4]. These proteins were subjected to *in vitro* phosphorylation by Cdk5–p25 purified from Sf9 cells [27]. Phosphorylation was detected on a FLA7000 Image Analyzer (GE Healthcare) after SDS-PAGE.

## 3. Results

### 3.1. Ataxin-2 is phosphorylated by Cdk5 in COS-7 cells

Ataxin-2 contains 47 (S/T)P Cdk5 minimum consensus sequences, with two preferred sequences (S/T)PX(K/R) at Ser132 and Thr580 (Genbank accession number; NP_002964) (Fig. 1A). We examined if ataxin-2 was phosphorylated by Cdk5 by co-expressing GFP-ataxin-2 with Cdk5–p25 in COS-7 cells. We used p25 C-terminal fragment for activation of Cdk5 in this study because of its high and constant activation of Cdk5 activity. The expression of ataxin-2 alone led to its detection at 160 kDa via Laemmli SDS-PAGE (Fig. 1B). Coexpression with Cdk5–p25, but not with kinase negative (kn) Cdk5 and p25, shifted the electrophoretic mobility slightly, to a higher position (Fig. 1B, arrows), which suggests phosphorylation by Cdk5. An *in vitro* kinase assay showed the direct phosphorylation of ataxin-2 by Cdk5 (Fig. 1C). These results indicate that ataxin-2 is a substrate of Cdk5.

### 3.2. Phosphorylation of the N-terminal and middle regions of ataxin-2 by Cdk5

Ataxin-2 is a large protein composed of 1313 amino acids (Fig. 1A). To determine which parts of ataxin-2 are phosphorylated, we divided ataxin-2 into three portions: the N-terminal fragment (NF, amino acids 1–507), the middle fragment (MF, amino acids 508–905), and the C-terminal fragment (CF, amino acids 906–1313), each of which contained 8, 22, and 17 (S/T)P sequences, respectively (Fig. 1A). These fragments were constructed as the GFP fusion as described in Section 2.

We coexpressed each of these fragments with Cdk5–p25 in COS-7 cells (Fig. 2A, wt). MF exhibited an upward shift in electrophoretic mobility when coexpressed with Cdk5–p25, whereas no changes were observed for NF and CF in Laemmli SDS-PAGE (Fig. 2A). Nevertheless, the expression levels of NF were greatly reduced to about 30% by coexpression with Cdk5–p25 (right panel of Fig 2A). MF was also reduced moderately to about 70% by Cdk5–p25. To determine if NF is phosphorylated by Cdk5–p25, we used the Phos-tag SDS-PAGE method, which enhances the phosphorylation-dependent mobility shift [13,18]. About half of NF proteins were shifted upward by coexpression with Cdk5–p25, but not by coexpression with knCdk5 (Fig. 2B, NF). MF exhibited an upward shift in the absence of Cdk5–p25, suggesting that MF is phosphorylated by endogenous kinase(s). The Cdk5-induced upward shift of MF was remarkable

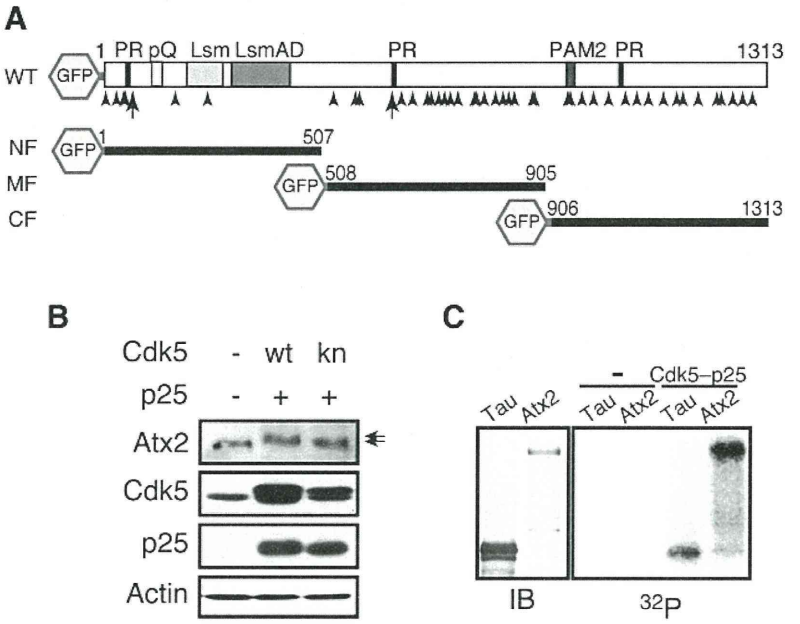


**Fig. 1.** Phosphorylation of ataxin-2 by Cdk5–p25. (A) Schematic representation of the ataxin-2 molecule and its fragments. Ataxin-2 is a large protein consisting of 1313 amino acids. The motif domains of ataxin-2, *i.e.*, the putative RNA-binding domain (Lsm), the Lsm-associated domain (LsmAD), the polyA-binding protein-interacting motif (PAM2), and three proline-rich (PR) domains, are indicated. The polyQ stretch (pQ) is located in the N-terminal region. There are 47 (S/T)P Cdk5 minimum phosphorylation consensus sequences (arrowheads) with two preferred consensus sequences, (S/T)PX(K/R) (arrows). Ataxin-2 was divided into three portions: NF, amino acids 1–507; MF, amino acids 508–905; and CF, amino acids 906–1313. All fragments were tagged with GFP at the N-terminus. (B) Coexpression of ataxin-2 and Cdk5–p25 in COS-7 cells. GFP-ataxin-2 was expressed in COS-7 cells alone or with Cdk5–p25 or kinase-negative (kn) Cdk5–p25. Ataxin-2, Cdk5, and p25 were detected by immunoblotting with anti-GFP, anti-Cdk5, and anti-p35/p25 antibodies. Actin was used as the loading control. (C) Phosphorylation of GFP-ataxin-2 by Cdk5 *in vitro*. GFP ataxin-2 was prepared from COS-7 cells by immunoprecipitation with anti-GFP antibody and phosphorylated by incubation without (-) or with Cdk5–p25 and [$\gamma$-$^{32}$P]ATP for 1 h at 37 °C. Incorporation of $^{32}$P was detected after SDS-PAGE. The microtubule-associated protein Tau was used as a positive control of phosphorylation. GFP-tau was prepared from COS-7 cells and phosphorylated by the same method as GFP-ataxin-2. Immunoblotting of GFP-ataxin-2 and GFP-tau is shown in left two lanes.

(Fig. 2B, MF), indicating the presence of multiple phosphorylation sites in MF. No mobility shift was induced in CF by coexpression with Cdk5–p25, although a Cdk5-independent shift was observed (Fig. 2B, CF). Direct phosphorylation of NF and MF by Cdk5 was confirmed by *in vitro* phosphorylation experiments using recombinant Cdk5–p25 and [$\gamma$-$^{32}$P]ATP. Both NF and MF were phosphorylated to the expected extent: weak and strong phosphorylation signals for NF and MF, respectively (Fig. 2C).

The expression levels of NF and MF were decreased remarkably and slightly, respectively, by coexpression with Cdk5–p25 (Fig. 2D). Many of the Cdk5 substrates are degraded by the proteasome [23,26]. To determine if the decrease in NF and MF expression also corresponded to proteasomal degradation, COS-7 cells expressing NF or MF were treated with the MG132 proteasome inhibitor. MG132 suppressed the decrease in the expression of ataxin-2 NF (Fig. 2D, left) or MF (Fig. 2D, middle). Quantification is shown in the right panel of Fig. 2D. Theses results indicate that the degradation of NF or MF is proteasome dependent.

### 3.3. The degradation of pathological ataxin-2-41Q is induced by phosphorylation by Cdk5

The control of the expression levels of pathological ataxin-2 is important to prevent disease development. Thus, we assessed the phosphorylation and degradation of mutant ataxin-2 with 41Q together with normal ataxin-2-22Q. We transfected ataxin-2-22Q (Fig. 3A) or 41Q (Fig. 3B) alone or with Cdk5–p25 into COS-7 cells. Coexpression of Cdk5–p25 shifted the electrophoretic mobility of ataxin-2-41Q and of ataxin-2-22Q. The levels of protein were decreased slightly (~25%) for ataxin-2-22Q and considerably (~60%) for ataxin-2-41Q (right panels of Fig. 3A and B). It was interesting that ataxin-2-41Q was reduced more than ataxin-2-22Q in the presence of Cdk5–p25. This decrease was suppressed by MG132, indicating the degradation by the proteasome. Considering that the expression of NF was extremely low in the presence of Cdk5–p25, there may be a degradation signal in the N-terminal region which is affected by phosphorylation. Both ataxin-2-22Q and -41Q appeared at a higher molecular weight region in the presence of MG132 (Fig. 3A and B), suggesting the preferential degradation of phosphorylated ataxin-2. These results suggest that full-length ataxin-2, either the normal 22Q or the toxic 41Q form, undergoes proteasomal degradation after phosphorylation by Cdk5.

## 4. Discussion

An intermediate or large polyQ expansion in the ataxin-2 protein represents a risk factor for ALS and causes SCA2, respectively [9,16,25,28]. However, neither the physiological functions nor the pathological mechanism of the protein are known. Here, we showed that ataxin-2 was phosphorylated by Cdk5. Phosphorylation occurred mainly in the middle region and, to a lesser extent, in the N-terminal region. Importantly, the degradation of ataxin-2 was induced by phosphorylation by Cdk5–p25. The present results suggest that Cdk5 controls the abundance of the ataxin-2 protein through proteasomal degradation in neurons.

Ataxin-2 has 47 (S/T)P possible phosphorylation sequences. There is only one report describing the phosphorylation of ataxin-2 in SY5Y cells, as assessed by metabolic $^{32}$P labeling [30]. Here, we demonstrated the phosphorylation of ataxin-2 using two methods: electrophoretic mobility shift on Phos-tag SDS-PAGE and phosphate labeling. The middle and N-terminal regions were highly and slightly phosphorylated by Cdk5, respectively. The C-terminal

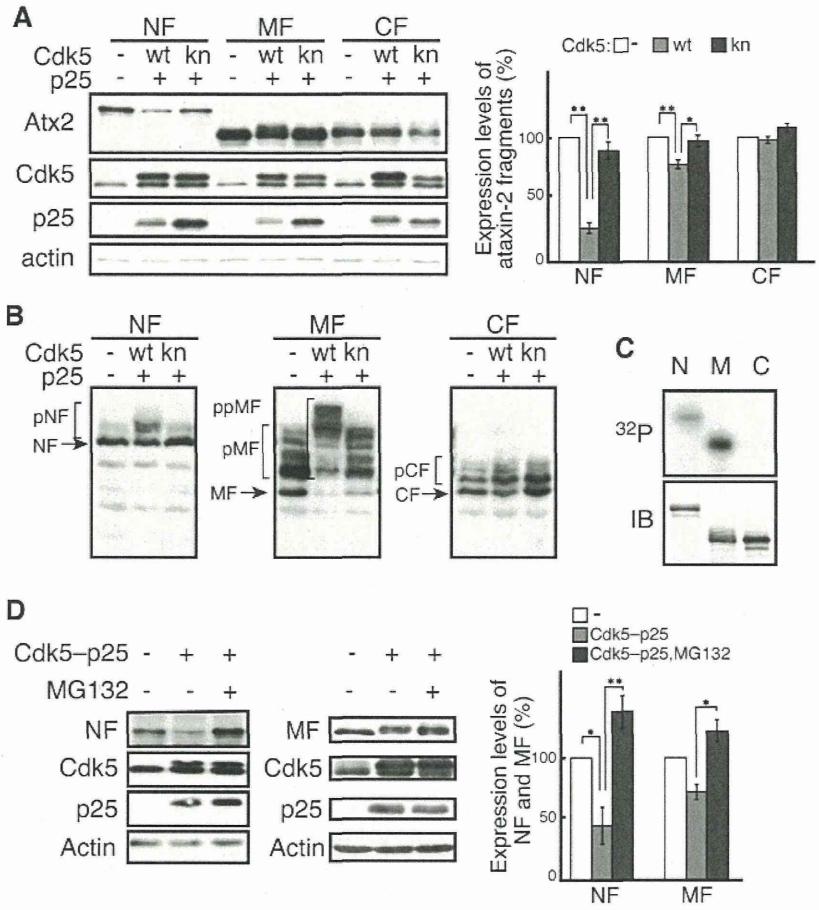


**Fig. 2.** Phosphorylation of ataxin-2 fragments by Cdk5. (A) Expression of ataxin-2 in COS-7 cells in the presence or absence of Cdk5–p25. The ataxin-2 fragment NF, MF, or CF was expressed alone (–) or with Cdk5–p25 or knCdk5–p25 in COS-7 cells. Ataxin-2, Cdk5, and p25 were detected by immunoblotting with anti-GFP, anti-Cdk5, and anti-p35/p25 antibodies. Actin was used as the loading control. Expression levels of ataxin-2 fragments are quantified and shown as the ratio to the control in the absence of Cdk5–p25 (right panel, means + s.e.m, $n = 3$, $^{*}p < 0.05$, $^{**}p < 0.01$ in Tukey's post hoc test). (B) Cdk5 phosphorylation of ataxin-2 fragments. Ataxin-2 NF, MF, or CF was expressed in COS-7 cells, and phosphorylation was examined by Phos-tag SDS-PAGE, followed by immunoblotting with an anti-GFP antibody. The band corresponding to unphosphorylated NF, MF, or CF is indicated by arrows. Bands corresponding to phosphorylated NF, MF, and CF (pNF, pMF, ppMF, and pCF) are indicated by brackets. In the case of MF, endogenous phosphorylation and further phosphorylation by Cdk5 are labeled differently as pMF and ppMF, for explicitness. (C) *In vitro* phosphorylation of ataxin-2 NF, MF, and CF by Cdk5. Ataxin-2 NF, MF, or CF was immunopurified from COS-7 cells with an anti-GFP antibody and was phosphorylated by incubation with Cdk5–p25 and [$\gamma$-$^{32}$P]ATP for 1 h at 37 °C. The incorporation of $^{32}$P is shown in the upper panel ($^{32}$P) and proteins are shown in the lower panel, as identified by immunoblotting with an anti-GFP antibody (IB). (D) Proteasomal degradation of ataxin-2 NF and MF. COS-7 cells expressing NF (left) or MF (middle) alone or with Cdk5–p25 were treated with or without the proteasome inhibitor MG132 for 2 h. NF, MF, Cdk5, and p25 were detected by immunoblotting with anti-GFP, anti-Cdk5, and anti-p35/p25 antibodies, respectively. Actin was used as the loading control. Quantification of NF and MF is shown in the right panel (means + s.e.m, $n = 3$, $^{*}p < 0.05$, $^{**}p < 0.01$ in Tukey's post hoc test).

region was not phosphorylated at all by Cdk5, even though it contains 17 (S/T)P sequences, which is comparable to MF and greater than that observed for NF. Other factors, such as conformation, may influence Cdk5-mediated phosphorylation. In addition, using Phos-tag SDS-PAGE, we observed the phosphorylation of the middle and C-terminal regions of the protein by an endogenous kinase in COS-7 cells. This phosphorylation may correspond to that detected by metabolic labeling [30].

Ataxin-2-41Q was prone to degradation by the proteasome to a greater extent than was ataxin-2-22Q (Fig. 3). It has been reported that the ataxin-2 immunoreactivity in SCA2 brain tissues is more intense than that found in normal brain tissues [14]. The increased concentration of pathological ataxin-2 may contribute to the development of SCA2. If so, it is very important to understand the mechanism that regulates the levels of the ataxin-2 protein in neurons. The degradation of ataxin-2 was induced by phosphorylation by Cdk5–p25. Among the three ataxin-2 fragments, NF exhibited the most remarkable Cdk5-dependent degradation. Phosphorylation in the N-terminal region may be a degradation signal, although the extent of phosphorylation observed was low. It has been reported that Parkin, which is an E3 ubiquitin ligase and the mutation of which induces Parkinson's disease [19], interacts with the N-terminal half of ataxin-2 and ubiquitinates it for degradation [15]. Parkin is phosphorylated at Ser131 by Cdk5, and an unphosphorylated mutant (S131A) of Parkin increases the inclusions of Parkin itself and of synphilin-1/$\alpha$-synuclein [5]. It will be interesting to determine if Parkin is involved in the Cdk5-dependent degradation of ataxin-2 in neuronal cells. We have to state that in COS-7 cells Parkin may not be an ubiquitin ligase of ataxin-2 because the expression is very low in COS-7 cells [2].

It is worth noting that Cdk5 plays a role in ameliorating the cytotoxicity of mutant huntingtin (mhtt), which is another polyQ protein. Cdk5 suppresses the formation of mhtt aggregates by reducing the production of the toxic N-terminal fragment by cleavage with caspases [21], or by microtubule destabilization [17]. Furthermore, Cdk5 renders striatal neurons resistant to DNA damage by phosphorylating wild-type htt [1]. The expression of Cdk5

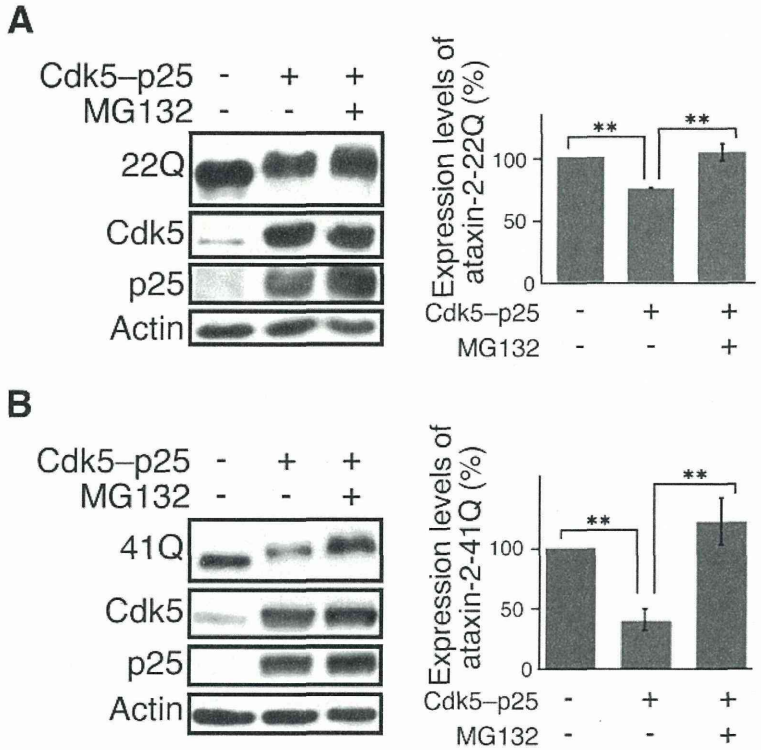


**Fig. 3.** Cdk5-dependent degradation of ataxin-2-41Q. COS-7 cells expressing GFP-ataxin-2, -22Q (A), or -41Q (B), and Cdk5–p25 were treated with (+) or without (−) MG132 for 8 h. Ataxin-2, Cdk5, and p25 were detected by immunoblotting with anti-GFP, anti-Cdk5, and anti-p35/p25 antibodies, respectively. Actin was used as the loading control. Quantification of ataxin-2-22Q and -41Q is shown in the right panel (means + s.e.m, $n = 3$, $n = 3$, $^{*}p < 0.05$, $^{**}p < 0.01$ in Tukey's post hoc test).

is reduced in the striatal medium-sized spiny neurons in Huntington's disease model mice [21]. It is possible that Cdk5 acts widely against the toxicity of polyQ proteins, including htt and ataxin-2. If so, the activity of Cdk5 is a therapeutic approach for polyQ neurodegenerative diseases.

## Acknowledgement

This work was supported in part by Grants-in-Aid for Scientific Research from MEXT of Japan (S.H.). We thank Dr. F Hayashi at Tokyo Metropolitan University for statistical analysis.

## References

[1] S.L. Anne, F. Saudou, S. Humbert, Phosphorylation of huntingtin by cyclin-dependent kinase 5 is induced by DNA damage and regulates wild-type and mutant huntingtin toxicity in neurons, J. Neurosci. 27 (2007) 7318–7328.
[2] H.C. Ardley, G.B. Scott, S.A. Rose, N.G.S. Tan, A.F. Markham, P.A. Robinson, Inhibition of proteasomal activity causes inclusion formation in neuronal and non-neuronal cells overexpressing Parkin, Mol. Biol. Cell 14 (2003) 4541–4556.
[3] A. Asada, N. Yamamoto, M. Gohda, T. Saito, N. Hayashi, S. Hisanaga, Myristoylation of p39 and p35 is a determinant of cytoplasmic or nuclear localization of active cyclin-dependent kinase 5 complexes, J. Neurochem. 106 (2008) 1325–1336.
[4] A. Asada, T. Saito, S. Hisanaga, Phosphorylation of p35 and p39 by Cdk5 determines the subcellular location of the holokinase in a phosphorylation-site-specific manner, J. Cell Sci. 125 (2012) 3421–3429.
[5] E. Avraham, R. Rott, E. Liani, R. Szargel, S. Engelender, Phosphorylation of Parkin by the cyclin-dependent kinase 5 at the linker region modulates its ubiquitin-ligase activity and aggregation, J. Biol. Chem. 282 (2007) 12842–12850.
[6] P.O. Bauer, A. Goswami, H.K. Wong, M. Okuno, M. Kurosawa, M. Yamada, H. Miyazaki, G. Matsumoto, Y. Kino, Y. Nagai, N. Nukina, Harnessing chaperone-mediated autophagy for the selective degradation of mutant huntingtin protein, Nat. Biotechnol. 28 (2010) 256–263.
[7] Z.H. Cheung, N.Y. Ip, Cdk5: a multifaceted kinase in neurodegenerative diseases, Trends Cell Biol. 22 (2012) 169–175.
[8] R. Dhavan, L.H. Tsai, A decade of CDK5, Nat. Rev. Mol. Cell Biol. 2 (2001) 749–759.
[9] A.C. Elden, H.J. Kim, M.P. Hart, A.S. Chen-Plotkin, B.S. Johnson, X. Fang, M. Armakola, F. Geser, R. Greene, M.M. Lu, A. Padmanabhan, D. Clay-Falcone, L. McCluskey, L. Elman, D. Juhr, P.J. Gruber, U. Rüb, G. Auburger, J.Q. Trojanowski, V.M. Lee, V.M. Van Deerlin, N.M. Bonini, A.D. Gilter, Ataxin-2 intermediate-length polyglutamine expansions are associated with increased risk for ALS, Nature 466 (2010) 1069–1075.
[10] X. Gong, X. Tang, M. Wiedmann, X. Wang, J. Peng, D. Zheng, L.A. Blair, J. Marshall, Z. Mao, Cdk5-mediated inhibition of the protective effects of transcription factor MEF2 in neurotoxicity-induced apoptosis, Neuron 38 (2003) 33–46.
[11] M. Hasegawa, M.J. Smith, M. Goedert, Tau proteins with FTDP-17 mutations have a reduced ability to promote microtubule assembly, FEBS Lett. 437 (1998) 207–210.
[12] S. Hisanaga, R. Endo, Regulation and role of cyclin-dependent kinase activity in neuronal survival and death, J. Neurochem. 115 (2010) 1309–1321.
[13] T. Hosokawa, T. Saito, A. Asada, K. Fukunaga, S. Hisanaga, Quantitative measurement of in vivo phosphorylation states of Cdk5 activator p35 by Phos-tag SDS-PAGE, Mol. Cell. Proteomics 9 (2010) 1133–1143.
[14] D.P. Huynh, M.R. Del Bigio, D.H. Ho, S.M. Pulst, Expression of ataxin-2 in brains from normal individuals and patients with Alzheimer's disease and spinocerebellar ataxia 2, Ann. Neurol. 45 (1999) 232–241.
[15] D.P. Huynh, D.T. Nguyen, J.B. Pulst-Korenberg, A. Brice, S.M. Pulst, Parkin is an E3 ubiquitin-ligase for normal and mutant ataxin-2 and prevents ataxin-2-induced cell death, Exp. Neurol. 203 (2007) 531–541.
[16] G. Imbert, F. Saudou, G. Yvert, D. Devys, Y. Trottier, J.M. Garnier, C. Weber, J.I. Mandel, G. Cancel, N. Abbas, A. Dürr, O. Didierjean, G. Stevanin, Y. Agid, A. Brice, Cloning of the gene for spinocerebellar ataxia 2 reveals a locus with high sensitivity to expanded CAG/glutamine repeats, Nat. Genet. 14 (1996) 285–291.
[17] S. Kaminosono, T. Saito, F. Oyama, T. Ohshima, A. Asada, Y. Nagai, N. Nukina, S. Hisanaga, Suppression of mutant Huntingtin aggregate formation by Cdk5/p35 through the effect on microtubule stability, J. Neurosci. 28 (2008) 8747–8755.
[18] E. Kinoshita, E. Kinoshita-Kikuta, K. Takiyama, T. Koike, Phosphate-binding tag, a new tool to visualize phosphorylated proteins, Mol. Cell. Proteomics 5 (2006) 749–757.
[19] T. Kitada, S. Asakawa, N. Hattori, H. Matsumine, Y. Yamamura, S. Minoshima, M. Yokochi, Y. Mizuno, N. Shimizu, Mutations in the parkin gene cause autosomal recessive juvenile parkinsonism, Nature 392 (1998) 605–608.
[20] I. Lastres-Becker, U. Rüb, G. Auburger, Spinocerebellar ataxia 2 (SCA2), Cerebellum 7 (2008) 115–124.
[21] S. Luo, C. Vacher, J.E. Davies, D.C. Rubinsztein, Cdk5 phosphorylation of huntingtin reduces its cleavage by caspases: implications for mutant huntingtin toxicity, J. Cell Biol. 169 (2005) 647–656.
[22] J.J. Magaña, L. Velázquez-Pérez, B. Cisneros, Spinocerebellar ataxia type 2: clinical presentation, molecular mechanisms, and therapeutic perspectives, Mol. Neurobiol. 47 (2013) 90–104.

[23] M.A. Morabito, M. Sheng, L.H. Tsai, Cyclin-dependent kinase 5 phosphorylates the N-terminal domain of the postsynaptic density protein PSD-95 in neurons, J. Neurosci. 24 (2004) 865–876.
[24] G.N. Patrick, L. Zukerberg, M. Nikolic, S. de la Monte, P. Dikkes, L.H. Tsai, Conversion of p35 to p25 deregulates Cdk5 activity and promotes neurodegeneration, Nature 402 (1999) 615–622.
[25] S.M. Pulst, A. Nechiporuk, T. Nechiporuk, S. Gispert, X.N. Chen, I. Lopes-Cendes, S. Pearlman, S. Starkman, G. Orozco-Diaz, A. Lunkes, P. DeJong, G.A. Rouleau, G. Auburger, J.R. Korenberg, C. Figueroa, S. Sahba, Moderate expansion of a normally biallelic trinucleotide repeat in spinocerebellar ataxia type 2, Nat. Genet. 14 (1996) 269–276.
[26] F. Roselli, P. Livrea, O.F. Almeida, CDK5 is essential for soluble amyloid β-induced degradation of GKAP and remodeling of the synaptic actin cytoskeleton, PLoS One 6 (2011) e23097.
[27] T. Saito, T. Konno, T. Hosokawa, A. Asada, K. Ishiguro, S. Hisanaga, p25/cyclin-dependent kinase 5 promotes the progression of cell death in nucleus of endoplasmic reticulum-stressed neurons, J Neurochem. 102 (2007) 133–140.
[28] K. Sanpei, H. Takano, S. Igarashi, T. Sato, M. Oyake, H. Sasaki, A. Wakisaka, K. Tashiro, Y. Ishida, T. Ikeuchi, R. Koide, M. Saito, A. Sato, T. Tanaka, S. Hanyu, Y. Takiyama, M. Nishizawa, N. Shimizu, Y. Nomura, M. Segawa, K. Iwabuchi, I. Eguchi, H. Tanaka, H. Tkahashi, S. Tsuji, Identification of the spinocerebellar ataxia type 2 gene using a direct identification of repeat expansion and cloning technique, DIRECT, Nat. Genet. 14 (1996) 277–284.
[29] S.B. Shelton, G.V. Johnson, Cyclin-dependent kinase-5 in neurodegeneration, J. Neurochem. 88 (2004) 1313–1326.
[30] V.J. Turnbull, E. Storey, V. Tarlac, R. Walsh, D. Stefani, R. Clark, L. Kelly, Different ataxin-2 antibodies display different immunoreactive profiles, Brain Res. 1027 (2004) 103–116.


RESEARCH PAPER

# Spreading of amyotrophic lateral sclerosis lesions—multifocal hits and local propagation?

Teruhiko Sekiguchi,[1] Tadashi Kanouchi,[2] Kazumoto Shibuya,[3] Yu-ichi Noto,[4] Yohsuke Yagi,[5] Akira Inaba,[6] Keisuke Abe,[7] Sonoko Misawa,[3] Satoshi Orimo,[6] Takayoshi Kobayashi,[7] Tomoyuki Kamata,[5] Masanori Nakagawa,[4] Satoshi Kuwabara,[3] Hidehiro Mizusawa,[1] Takanori Yokota[1]

► Additional material is published online only. To view please visit the journal online (http://dx.doi.org/10.1136/jnnp-2013-305617).

For numbered affiliations see end of article.

**Correspondence to**
Dr Takanori Yokota, Department of Neurology and Neurological Science, Graduate School, Tokyo Medical and Dental University, 1-5-45 Yushima Bunkyo-ku, Tokyo 113-8519, Japan; tak-yokota.nuro@tmd.ac.jp

Received 16 April 2013
Revised 27 June 2013
Accepted 17 July 2013
Published Online First 11 September 2013

## ABSTRACT

**Objective** To investigate whether or not the lesions in sporadic amyotrophic lateral sclerosis (ALS) originate from a single focal onset site and spread contiguously by prion-like cell-to-cell propagation in the rostrocaudal direction along the spinal cord, as has been hypothesised (the 'single seed and simple propagation' hypothesis).

**Methods** Subjects included 36 patients with sporadic ALS and initial symptoms in the bulbar, respiratory or upper limb regions. Abnormal spontaneous activities in needle electromyography (nEMG)—that is, fibrillation potentials, positive sharp waves (Fib/PSWs) or fasciculation potentials (FPs)—were compared among the unilateral muscles innervated by different spinal segments, especially between the T10 and L5 paraspinal muscles, and between the vastus medialis and biceps femoris. Axon length and the proportion of muscle fibre types, which are both related to motoneuronal vulnerability in ALS, are similar in the paired muscles.

**Results** Fourteen of 36 patients showed a non-contiguous distribution of nEMG abnormalities from the onset site, with skipping of intermediate segments. In eight of them, the non-contiguous pattern was evident between paired muscles with the same motoneuronal vulnerability. The non-contiguously affected lumbosacral lesions involved motoneuron columns horizontally or radially proximate to one another, appearing to form a cluster in four of the eight patients. FPs, known to precede Fib/PSWs, were shown more frequently than Fib/PSWs in all the lumbosacral segments but L5, suggesting that 2nd hits occur at L5 and then spread to other lumbosacral segments.

**Conclusions** In sporadic ALS, the distribution of lower motoneuron involvement cannot be explained by the 'single seed and simple propagation' hypothesis alone. We propose a 'multifocal hits and local propagation' hypothesis instead.

## INTRODUCTION

Amyotrophic lateral sclerosis (ALS) is an incurable progressive neurodegenerative disease in which both the upper (UMN) and lower motoneurons (LMN) are diffusely involved at the end. Recent biological studies have demonstrated the remarkable concept of 'prion-like propagation' of pathogenic proteins, such as tau or α-synuclein, in neurodegenerative diseases.[1 2] According to this hypothesis, the pathogenic proteins are transferred from diseased cells to neighbouring healthy cells; this intercellular transfer then leads to spreading of the lesion. In ALS, in vitro studies have indicated that newly formed aggregates of SOD1, TDP-43 or toxic RNA conformation can act as templates for the subsequent misfolding of the respective native proteins,[3–5] and that aggregated SOD1 can be intercellularly transferred in cultured cells.[6] These suggest that the mechanism of prion-like cell-to-cell propagation also underlies the progression of ALS.

The clinical symptoms of most ALS patients start focally, which had already been confirmed both electrophysiologically[7] and pathologically.[8 9] As we have reviewed in the previous article,[10] recent clinical observations have demonstrated that the clinical symptoms spread contiguously from the onsets into the following broadly divided body regions: the bulbar region, upper limbs, trunk and lower limbs.[11–14] This has prompted us to suppose that ALS lesions simply propagate from a single 'seed' to adjacent cells in a domino-like manner (ie, the 'single seed and simple propagation' hypothesis). Alternatively, it can rest on anatomical proximity with the spreading of ALS lesion from the onset site by diffusion of soluble toxic factors in the extracellular matrix.[15] On the other hand, up to about 30% of sporadic ALS patients have also been found to show non-contiguous spread of symptoms from the bulbar region to the lower limbs or vice versa, skipping the upper limbs and trunk.[14 16] However, compensatory re-innervation by the remaining motoneurons can mask the manifestation of clinical signs until more than one-third of the LMNs for a given muscle are lost.[17] Therefore, whether the lesions actually spread non-contiguously among the spinal segments remains unclear.

Needle electromyography (nEMG) can sensitively detect LMN involvement from each segment separately, even in the presymptomatic stage. For this reason, it is a powerful method for investigating whether or not ALS lesions spread contiguously along the spinal segments. In this study, we used nEMG in the early stage of ALS to demonstrate that LMN involvement cannot be necessarily explained by the 'single seed and simple propagation' hypothesis. We then propose a hypothesis of 'multifocal hits and local propagation.'

**To cite:** Sekiguchi T, Kanouchi T, Shibuya K, *et al*. *J Neurol Neurosurg Psychiatry* 2014;**85**:85–91.

## SUBJECTS AND METHODS

### Subjects

We designed this study to investigate whether LMN involvement in sporadic ALS spreads contiguously in the rostrocaudal direction from the onset site. Therefore, of 66 consecutive patients with suspected ALS referred to our hospitals from March 2011 to April 2012, 14 patients with lower limb onset were excluded. One patient with a family history of ALS was also excluded. Forty-two of the remaining 51 patients met the revised El Escorial criteria[18] for clinically definite, clinically probable or clinically probable laboratory-supported ALS, although two patients were excluded because their MRIs indicated lumbar spinal disease, which can influence the results of nEMG. Thus, 40 sporadic ALS patients with bulbar, upper limb, or respiratory symptoms at onset were ultimately included in this study. None of these 40 patients had diabetes or any other complicating neuropathies, which were confirmed by nerve conduction studies (performed on their unilateral median, ulnar, tibial, peroneal and sural nerves).

### Selection of muscles to be examined

Motoneurons with longer axons,[19 20] larger motoneurons[9] and fast-fatigable motoneurons[21] have been described as more vulnerable to damage from ALS. If the pathological process begins at the same time in individual motoneurons with different degrees of vulnerability, then motoneurons that are more vulnerable will degenerate faster than those that are more resistant. Thus the pattern of nEMG abnormalities should be influenced by differences in motoneuronal vulnerability. Therefore, to establish adequate milestones for lesion spreading, we selected two pairs of muscles innervated from different spinal segments but with similar degrees of motoneuronal vulnerability; that is, the length of the innervating motor axons and the ratio of type I muscle fibres differ little between the paired muscles (see online supplementary figure S1). One pair—T10 paraspinalis (T10PS; type I fibre ratio: 62.0% in men, 67.8% in women) and L5 paraspinalis (L5PS; 63.6–65.0%)—was selected from the trunk.[22] The other pair—the deep layer of the vastus medialis (VM) (innervating segment: L3/4; type I fibre ratio: 61.5%) and the long head of the biceps femoris (BF; L5/S1, mainly S1; 66.9%)—was selected from the thigh.[23–27]

If a focal ALS lesion spreads contiguously in the rostrocaudal direction along the spinal segments, nEMG abnormalities in the paired muscles should be found in the muscle innervated by the rostral segment earlier than in the muscle innervated by the caudal segment (the 'contiguous pattern' in online supplementary figure S1). On the other hand, if the abnormalities are observed only in the muscle innervated by the caudal segment while the muscle of the rostral segment remains intact (the 'non-contiguous (skipping) pattern' in online supplementary figure S1), the results cannot be attributed to differences in motoneuronal vulnerability. We also examined the first dorsal interosseous (FDI; mainly innervating segment: C8), L3 paraspinalis (L3PS), rectus femoris (RF; L3/4), tibialis anterior (TA; L4/5, mainly L5) and medial head of the gastrocnemius (GC; S1/2, mainly S1).[23–26]

### Needle electromyography

Spontaneous EMG activities were detected with a conventional concentric needle electrode (recording surface area: 0.3 $mm^2$) in the above-mentioned muscles on the ipsilateral side of symptom onset in the upper limb onset patients and on the right side in the patients with bulbar or respiratory onset. For evaluation of paraspinal muscles, we examined the multifidus muscles, which are innervated by a single segment.[28]

Fibrillation potentials and positive sharp waves (Fib/PSWs) were explored at 10 different sites in each muscle. Fib/PSWs were diagnosed to be pathological only when they were identified at more than two different sites within the muscle. The fasciculation potential (FP) was defined as a potential that was similar in shape to the motor unit potential (MUP) and fired in a highly irregular pattern, often with a clustering of discharges. We identified FPs only when potentials of the same shape appeared at least twice. To detect FPs, we observed spontaneous activity at one site in each muscle for 60–90 s, which is sufficiently long enough to confirm the reproducibility of FPs.[29] Any persistence of voluntary MUPs was considered to render the identification of FPs impossible. We considered the examined muscles to be involved if Fib/PSWs, FPs or both were observed. Considering their higher objectivity beyond multicentre and burdens of patients, only spontaneous activities were adopted to prove LMN involvements in this study.

All EMG examinations were performed by proficient electromyographers with at least 5 years of professional EMG experience (TS, TK, KS and YN).

### Data analysis

Frequencies of the presence of abnormal spontaneous EMG activity were compared among the examined muscles by performing multiple comparisons with Fisher's exact probability test and the p value adjustment method of Holm. p Values less than 0.05 were considered to be significant.

### Standard protocol approvals, registrations and patient consents

The local ethics committees of Tokyo Medical and Dental University School of Medicine, Chiba University Graduate School of Medicine, Kyoto Prefectural University of Medicine, Musashino Red Cross Hospital, Kanto Central Hospital and Nakano General Hospital approved this study. All patients gave us informed consents for the procedures.

## RESULTS

Of the 40 patients with sporadic ALS included in this study, we ultimately analysed data from 36 patients (23 men, 13 women) because sufficient data for the paired paraspinal and thigh muscles were not obtained in 4 patients. The ages of 36 patients ranged from 41 years to 79 years (mean 63.3). The diagnoses were definite ALS in 8 patients, probable in 14 and probable-laboratory-supported in 14 according to the revised El Escorial criteria. Symptom onset occurred in the bulbar region in 10 patients, in the upper limb in 25 patients and as respiratory symptoms in 1 patient. The mean duration from symptom onset to the nEMG study was 16.9 months (range 3–84).

The full nEMG data for the 36 patients are shown in figure 1, online supplementary figure S2A,B. Abnormal spontaneous EMG activity was present in the FDI of all 36 patients. The distribution patterns of nEMG abnormalities among the spinal segments could be divided into three types: diffuse, contiguous and non-contiguous (skipping) patterns. The diffuse pattern was observed in 19 patients (53%); of these, 13 (patients 1–13) showed abnormal nEMG findings at all examined muscles and 6 (patients 14–19) showed abnormalities at every examined spinal segment, although not at all muscles. The contiguous pattern was found in three patients (8.3%; patients 20–22) in whom abnormal findings were detected in all examined segments except S1—the most remote segment from the onset site. One

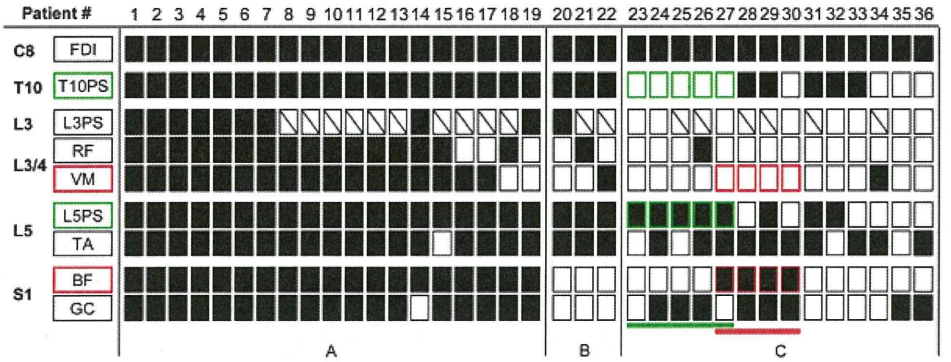


**Figure 1** Distribution patterns of needle electromyography (nEMG) abnormality in all patients. Closed squares: abnormal spontaneous EMG activity present. Open squares: abnormal spontaneous EMG activity absent. Squares with oblique line: data not available. (A) Diffuse pattern. (B) Contiguous pattern. (C) Non-contiguous (skipping) pattern. Note that the rostrally absent and caudally present spontaneous activity pattern between paired muscles with the same motoneuronal vulnerability is evident in the paraspinal muscle pair (green, patients 23–27) and the thigh muscle pair (red, patients 27–30) in 8 of 14 patients with the skipping pattern. The non-contiguous (skipping) pattern was present in both muscle pairs in patient 27.

of these three patients (patient 22) also showed the contiguous pattern in the thigh muscle pair; that is, an abnormality was evident in VM but not in BF. The non-contiguous (skipping) pattern was found in 14 patients (39%; patients 23–36), in whom abnormal spontaneous activities were detected from C8 to more caudal segments with skipping of intermediate segments such as T10 or L3/4. Representative nEMG findings of the non-contiguous pattern in a patient with bulbar onset (patient 27) are shown in figure 2.

Eight of the 14 patients also exhibited the non-contiguous pattern in the paired muscles; of these, five (patients 23–27) showed the pattern in the paraspinal muscle pair (involvement of L5PS with skipping of T10PS) (table 1A), four (patients 27–30) showed the pattern in the thigh muscle pair (involvement of BF innervated by S1 with skipping of VM innervated by L3/4) (table 1B). One of the eight patients (patient 27) showed this pattern in both pairs.

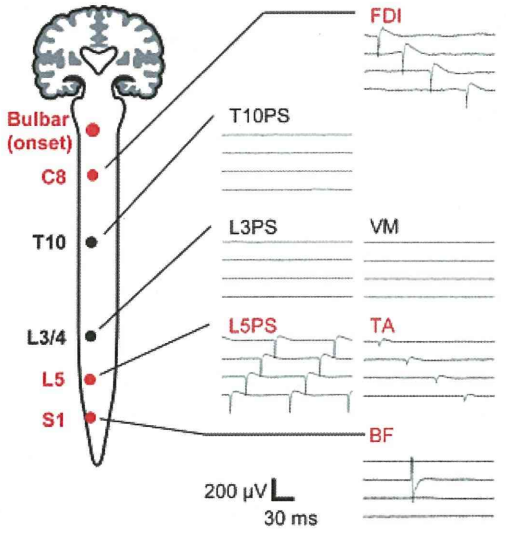


**Figure 2** Representative needle electromyography (nEMG) finding in the patient with non-contiguous pattern. nEMG finding of patient 27 whose onset was bulbar symptoms. Positive sharp waves (first dorsal interosseous (FDI), L5PS and tibialis anterior (TA)) or a fasciculation potential (biceps femoris (BF)) are present with skipping of the muscles innervated by intermediate segments. Note that the non-contiguous (skipping) distribution pattern is evident between the muscles of the paraspinal (T10PS and L5PS) and thigh (vastus medialis (VM) and BF) pairs. Red type indicates nEMG abnormalities.

In order to consider whether there is a local propagation of the non-contiguously affected lumbosacral lesion, we used schematics to examine the anatomical distributions of the involved motoneuron pools of the lumbosacral muscles in the eight patients who exhibited the skipping pattern in the paired muscles (figure 3).[23–26 30 31] The involved motoneuron pools were located in close horizontal or radial proximity to one another in five patients (patients 26–30) and appeared to form a cluster in four patients (patients 27–30). By contrast, the involved motoneuron pools were not horizontally contiguous in two patients (patients 24–25). The one remaining patient (patient 23) had only one lesion in the lumbosacral muscles.

Excluding FDI, which was involved in all patients, the percentage of patients with nEMG abnormalities was the highest in TA (13/17, 76.5%) and L5PS (11/17, 64.7%) and was the lowest in RF and VM (2/17, 11.8%) (figure 4). Pairwise comparisons among the muscles showed statistically significant differences in proportions between the muscles innervated by L3/4 and L5: RF and TA (p=0.01), RF and L5PS (p=0.03), VM and TA (p=0.01), and VM and L5PS (p=0.03). There were no

**Table 1** Frequencies of nEMG abnormality patterns in paired muscles among 14 patients with a non-contiguous (skipping) pattern

| | | | | |
|---|---|---|---|---|
| (A) The patterns in the paraspinal muscle pairs | | | | |
| FDI (C8) | + | + | + | + |
| T10PS | – | + | + | – |
| L5PS | – | – | + | + |
| Number of patients | 4 | 2 | 3 | 5 |
| (B) The patterns in the thigh muscle pairs | | | | |
| FDI (C8) | + | + | + | + |
| VM (L3/4) | – | + | + | – |
| BF (S1) | – | – | + | + |
| Number of patients | 9 | 1 | 0 | 4 |

+, abnormal spontaneous EMG activities present; –, abnormal spontaneous activities absent; BF, biceps femoris; FDI, first dorsal interosseous; T10PS, T10 paraspinalis; L5PS, L5 paraspinalis; VM, vastus medialis.

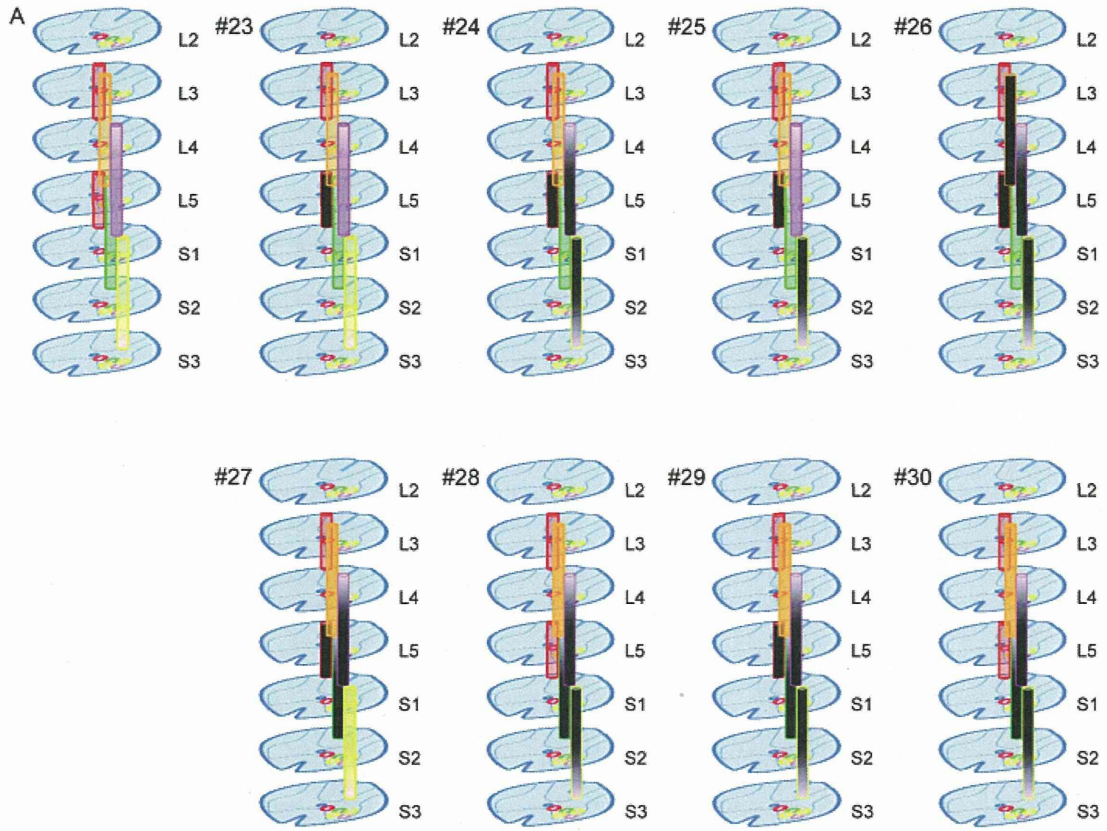


**Figure 3** Schematic diagrams of motoneuron pools of the examined muscles in the lumbosacral cord (A) and their patterns of involvement in eight patients showing the non-contiguous (skipping) pattern in the paired muscles (patients 23–30). The locations of motoneuron pools innervating each muscle were taken from refs [23–26 30] and [31]. Note that the involved motoneuron pools (darkly shaded) appear to neighbour one another in 3-dimensional anatomy, and appear to form a cluster for four patients (patients 27–30) in particular. VM (orange column), vastus medialis deep layer; RF (orange column), rectus femoris; L3 PS (upper red column), paraspinal muscle at L3 level; TA (pink column), tibialis anterior; L5 PS (lower red column), paraspinal muscle at L5 level; BF (green column), biceps femoris long head; GC (yellow column), gastrocnemius medial head.

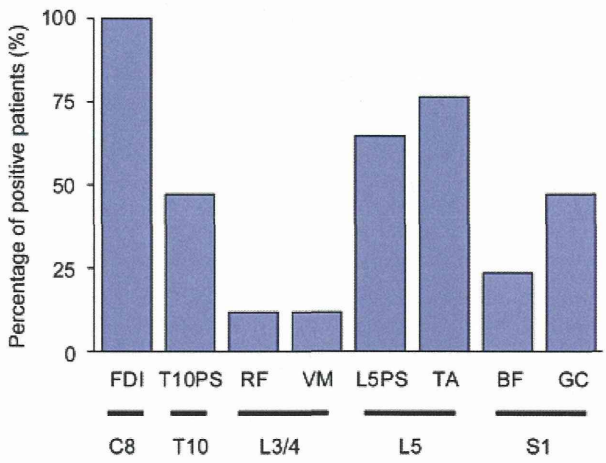


**Figure 4** Frequency of needle electromyography abnormality of each muscle in the patients with contiguous and non-contiguous distribution patterns. With the exception of first dorsal interosseous (FDI) which, as the most rostral muscle, was affected in all patients, the highest frequencies were found in the muscles innervated by L5 and the lowest in the muscles innervated by L3/4. The differences were statistically significant ($p<0.05$, Fisher's exact probability test using the p value adjustment method of Holm). Note that the frequencies are almost same between L5PS and tibialis anterior (TA).

statistically significant differences in other pairs of muscles except those including FDI.

We also investigated and compared the frequency of Fib/PSWs and that of FPs in every muscle of all included patients (figure 5). Fib/PSWs were more frequently observed than FPs in FDI (C8), which was the onset region in most of the included patients. To the contrary, FPs were dominantly observed than Fib/PSWs in RF or VM (L3/4) and BF or GC (S1), away from the onset region. However, TA and L5PS, both of which are innervated by L5, showed Fib/PSWs less rarely than FPs.

## DISCUSSION

We investigated whether the involvement of LMNs in sporadic ALS spreads contiguously in the rostrocaudal direction from the onset site. If prion-like propagation underlies the progression of ALS and the disease pathology in the first focal lesion propagates to adjacent cells in a cell-to-cell domino-like manner (the 'single seed and simple propagation' hypothesis) (see online supplementary figure S3A), involved LMNs should be distributed contiguously from the onset site.

Our nEMG study revealed that more than 50% of patients showed diffuse patterns. They showed weakness or muscle atrophy in lumbosacral regions more frequently than the rest (79% vs 29%). Therefore, they seemed to be in later stages of the disease.

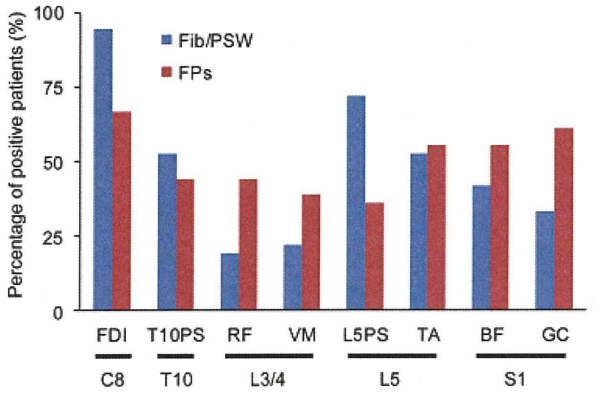


**Figure 5** The comparison of frequencies between fibrillation potentials, positive sharp waves (Fib/PSWs) and fasciculation potentials (FPs) of each muscle in all patients. Blue bar: Fib/PSWs, Red bar: FPs. FPs, known to precede Fib/PSWs, were shown more frequently than Fib/PSWs in the all lumbosacral segments but L5, suggesting that L5 segment was involved earlier than other lumbosacral segments.

In 14 of 17 patients, after excluding patients with the diffuse pattern, the abnormalities were distributed non-contiguously from the onset site, with skipping of intermediate spinal segments. The non-contiguous distribution of nEMG abnormalities may merely represent false-negative nEMG results in the 'skipped' segments where LMNs have in fact been involved. Two kinds of false negatives are conceivable: that based on methodological limitations, and that due to the time lag from molecular disease onset. First, given that a needle electrode has a limited pick-up area, evaluating all motor units (MU) in a muscle is practically impossible. Second, a time lag must exist because many molecular changes occur before they reach a threshold at which spontaneous EMG activities can be detected. Individual LMNs have different vulnerabilities in ALS;[9 19–21] more vulnerable LMNs will degenerate faster than more resistant ones even if the pathological molecular process begins simultaneously. Therefore, the failure to detect abnormal EMG activities in skipped spinal segments may simply have been caused by the lower vulnerability of neurons at these sites, if less vulnerable LMNs are radially sandwiched by the highly vulnerable LMNs of more rostral and caudal segments.

However, we consider it unlikely that they alone could produce the non-contiguous pattern. The sensitivities for detecting spontaneous EMG activity should be very similar in the two thigh muscles (VM and BF) and in the paraspinal muscles (T10 and L5) we examined. First, this is because the total number of insertions was fixed in every muscle by the same examiner. Second, the motoneuronal vulnerabilities as well as the sensitivities are expected to be nearly identical between the paired muscles because the lengths of their innervating motor axons are very similar and they have similar proportions of type I/II muscle fibres. Taken together, the probability of false negatives should be nearly same between the paired muscles. Therefore, the segmental distribution of ALS lesions can be non-contiguous along the spinal cord in the early stage of the disease (see online supplementary figure S3B).

Krarup claimed that abnormal spontaneous activities in nEMG are not as sensitive as changes in MUPs.[32] We have searched these chronic neurogenic changes in VM/RF of the four patients who showed non-contiguous pattern in thigh pair of muscles. Although one patient (patient 28) showed polyphasic MUPs in RF, the other three patients are still classified as non-contiguous pattern with evaluating chronic changes, and therefore, our conclusion remains unchanged. In fact, which kind of neurogenic changes appears the earliest in nEMG of ALS patients still remains controversial. Recently, de Carvalho *et al*[33] have reported that FPs are the earliest changes in ALS patients.

Both the spreading mechanisms of toxic factors, namely, simple diffusion of soluble toxic factors and cell-to-cell propagation from the only onset site are inconsistent with these non-contiguous distributions. The former mechanism should show abnormalities in anatomically proximal segments to onsets such as T10/L3 earlier than L5/S1. Assuming the latter mechanism, it is important to note that the lateral motor columns of the anterior horn innervating distal limb muscles are not structurally contiguous between the cervical and lumbosacral spinal cords.[30] By contrast, the medial motor column, which innervates axial muscles, extends contiguously from the lower medulla to the lumbar spinal cord. This indicates that regional spread from FDI to TA needs to have three steps; (1) disease transfer from lateral to medial motor column in cervical segment, (2) caudal propagation along the medial column and (3) disease transfer from medial to lateral motor column in lumbosacral segments. If ALS lesions spread along the medial column in the rostrocaudal direction by cell-to-cell propagation, our results showing the skipping of T10PS or L3PS in 11 of the 14 patients with non-contiguous pattern cannot be explained. Taken together, whatever mechanisms can underlie the consequent spread, we conclude that ALS progression is not explained by single onset site, but by multiple onset sites. This speculation is consistent with the fact that there are ALS patients who have onsets in two regions simultaneously.[14]

Rostral lesions were found to spread significantly more frequently to the TA and L5PS than L3/4 innervating muscles. Other investigators also demonstrated that abnormal spontaneous EMG activities were detected more frequently at the TA than at the quadriceps in ALS.[34 35] It is noteworthy that the L5PS was also highly involved in our study. Some electromyographers claim that the paraspinalis at the lower lumbar spine may show Fib/PSWs even in healthy subjects.[36] However, Fib/PSWs were not detected in normal subjects who did not have any abnormality of the lumbar spine on MRI,[37] and we also selected ALS patients without lumbar spine abnormalities on MRI. The fact that the involvement was almost identical between the TA and L5PS was unexpected, although a previous report showed a similar result in the early stage of ALS,[38] because LMNs of L5PS are generally considered less vulnerable than those of TA in ALS; LMNs innervating paraspinal muscles have shorter axons and smaller cell bodies than LMNs innervating distal muscles. These considerations imply a horizontal spread of ALS pathology from the more vulnerable neurons innervating the TA to the less vulnerable neurons innervating the L5PS within the L5 segment.

Another possible explanation for the frequent involvement of LMNs in the TA and L5PS is that L5 itself as a segment might be more vulnerable to ALS than other lumbosacral segments. ALS patients have lumbar spondylosis more frequently than the general population at corresponding ages,[39 40] although lumbar spondylosis was carefully excluded in our study by detailed MRI examinations. The L5 segment accounted for 90.3% of 112 vertebrae in Japanese patients with lumbar spondylosis.[40] Daily repetitive movements of the lumbar spine may cause weight-bearing biomechanical stresses particularly on L5, possibly inducing chronic minor trauma of the nerve root. Experimentally,